

Tetra-2,3-pyrazinoporphyrazines with Externally Appended Pyridine Rings.

17. Photosensitizing Properties and Cellular Effects of Zn^{II} Octacationic and Zn^{II}/Pt^{II} Hexacationic Macrocyces in Aqueous Media: Perspectives of Multimodal Anticancer Potentialities

Elisa Viola,^{§*} Maria Pia Donzello,^{§*} Fabiola Sciscione,[§] Koush Shah,[#] Claudio Ercolani,[§] and Giuseppe Trigiane^{**}

[§] Dipartimento di Chimica, Università Sapienza, P.le A. Moro 5, 00185 Roma, Italy

[#] Centre for Cutaneous Research, Queen Mary University of London, 4 Newark Street, London E1 2AT, U.K.

KEYWORDS

Positively charged pyrazinoporphyrazine macrocyces; photosensitizing activity in anticancer photodynamic therapy; antitumoral *in vitro* tests.

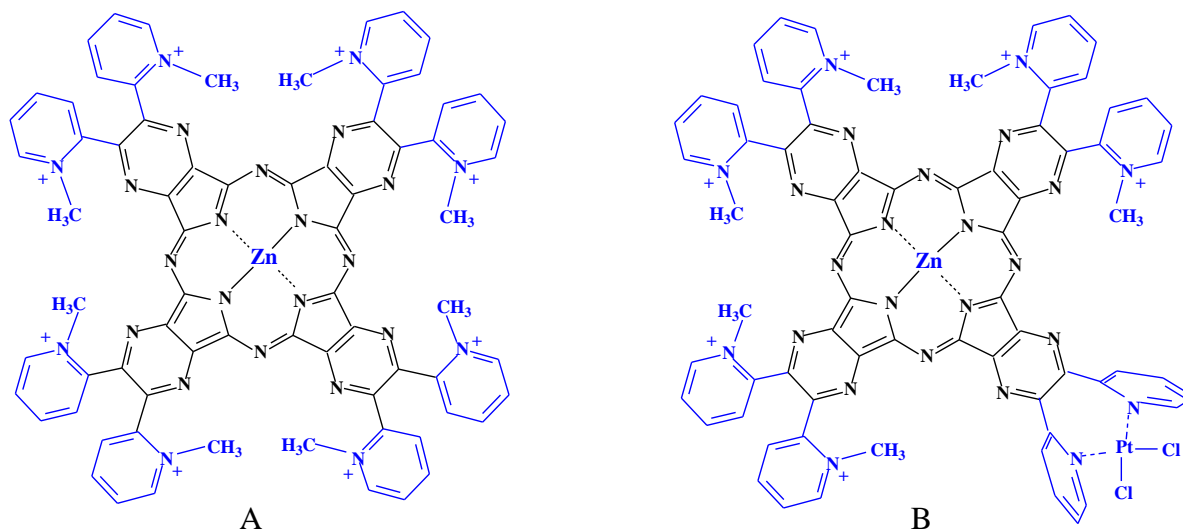
Abstract

The photosensitizing activity of two multiply charged porphyrazine derivatives, ie. the Zn^{II} species [(CH₃)₈LZn]⁸⁺ and the Zn^{II}/Pt^{II} heterobimetallic complex [(PtCl₂)(CH₃)₆LZn]⁶⁺ (neutralized by I⁻ ions; L = tetrakis-2,3-[5,6-di(2-pyridyl)pyrazino]porphyrazinatodianion) has been examined in the water medium in the presence of SDS under experimental conditions in which the two species are present exclusively in their monomeric form. The determined quantum yield values (Φ_{Δ}) for both complexes, of interest in photodynamic therapy (PDT), are 2.3-2.5 higher than that of the aluminium compound PcAlS_{mix} (Photosens[®]) used as the reference standard, an encouraging result for the application of the two cationic species as anticancer curative drugs in PDT. Investigation was also extended to explore the cellular effects on the melanoma C8161 and the oral squamous carcinoma CA-1 cell lines like viability, cellular uptake, cell death modality and cell cycle distribution experiments. The IC₅₀ values for the Zn^{II} and Zn^{II}/Pt^{II} cations are consistently lower than those of the reference standard, thus the degree of efficiency as anticancer agents being in the order octacation >> hexacation > PcAlS_{mix}. A large prevalence of apoptosis with respect to necrosis is observed for both charged complexes. Thus, all achieved information

from photoactivity and *in vitro* tests in water solution further enhance perspectives for the application of the two Zn^{II} cation [(CH₃)₈LZn]⁸⁺ and the related Zn^{II}/Pt^{II} analog [(PtCl₂)(CH₃)₆LZn]⁶⁺ as potential bi-multimodal anticancer drugs.

Introduction

As previously reported,¹ the tetrapyrazinoporphyrazine octacationic macrocycle [(CH₃)₈LZn]⁸⁺ (Scheme 1A) and the related dimetallic hexacation [(PtCl₂)(CH₃)₆LZn]⁶⁺ (both neutralized by I⁻ ions), this latter peripherally bearing one cis-platin-like functionality (Scheme 1B), are able to act as photosensitizers for the generation of singlet oxygen, ¹O₂, the main cytotoxic agent in photodynamic therapy (PDT), a well known anticancer curative modality.² Measurements of ¹O₂ quantum yields (Φ_Δ) were carried out prevalently in dimethylformamide (DMF) solution as in this low-donor non-aqueous solvent the compounds are present in their monomeric form, thus in the nearly complete absence of aggregation. The achieved Φ_Δ values (0.39-0.46) obtained in preacidified DMF ([HCl]: 1·10⁻⁴ M)^{1b} closely approach those reported in the literature (0.4-0.6) in the same solvent on Zn^{II} phthalocyanine³ or porphyrazine⁴ analogues which are among the most investigated photosensitizers because of their metal closed-shell electronic configuration.



Scheme 1: Schematic representation of the octacation [(CH₃)₈LZn]⁸⁺ (A) and the hexacation [(PtCl₂)(CH₃)₆LZn]⁶⁺ (B) (L = tetrakis-2,3-[5,6-di(2-pyridyl)pyrazino]porphyrazinatodianion).

Water solubility of the two charged complexes as the iodide salts [(CH₃)₈LZn](I₈) and [(PtCl₂)(CH₃)₆LZn](I₆) (isolated as hydrated species) allowed to examine, in K⁺ rich water

solutions, the interaction of the two cations $[(\text{CH}_3)_8\text{LZn}]^{8+}$ and $[(\text{PtCl}_2)(\text{CH}_3)_6\text{LZn}]^{6+}$ with a telomeric G-quadruplex structure (G4).⁵ For both species it could be established that, although in the presence of aggregation (equilibrium monomer/dimer), interaction of the monomeric form with G4 occurs, with formation of a very stable sandwich-type structure complex/G4 with 2:1 stoichiometry with stabilization of the G4 structure in its “parallel” form. A more complex type of interaction occurs for the $\text{Zn}^{\text{II}}/\text{Pt}^{\text{II}}$ hexacation with a double strand model of a B-DNA structure.⁶

Based on the available information on the two species $[(\text{CH}_3)_8\text{LZn}](\text{I}_8)$ and $[(\text{PtCl}_2)(\text{CH}_3)_6\text{LZn}](\text{I}_6)$ it was believed useful to study their photoactivity in water in the absence of disturbing aggregation, which, as well known,^{2d,3c,7} reduces the singlet and triplet excited state lifetimes of the macrocycles and hence $^1\text{O}_2$ production. Moreover, it was also required to provide qualified support to the potentialities in terms of multimodal anticancer activity by performing experiments on the cellular effects of the two multicharged species.

In the present contribution studies on the photoactivity of the cations $[(\text{CH}_3)_8\text{LZn}]^{8+}$ and $[(\text{PtCl}_2)(\text{CH}_3)_6\text{LZn}]^{6+}$ were conducted in water solution in the presence of sodium dodecyl sulphate (SDS), under experimental conditions which determine the occurrence of the species *exclusively* in their monomeric form. The obtained results are discussed for the two cations in strict relationship with data known from the literature for the widely studied Al-phthalocyanine photosensitizer $\text{PcAlS}_{\text{mix}}$ (Photosens[®]).⁷ Besides, in order to test the therapeutic potential of the two multicharged species in an appropriate biological setting, *in vitro* experiments were carried out on two cancer cell lines, C8161 (malignant melanoma) and CA-1 (oral squamous cell carcinoma). The experiments were aimed at characterizing the two cations in terms of a) IC_{50} , b) cellular uptake, c) cell death modality and d) cell cycle phase distribution. The obtained results are also presented and illustrated in detail.

Experimental Section

Solvents and Reagents. Reagents (Phthalocyanine aluminium chloride, PcAlCl ; 9,10-Anthracenediyl-bis(methylene)malonic acid; sodium dodecyl sulphate, SDS) and non aqueous solvents (pyridine; dimethylsulfoxide, DMSO; dimethylformamide, DMF) were purchased from Sigma Aldrich. H_2O Millipore was used as solvent. $\text{PcAlS}_{\text{mix}}$ was prepared locally and its

behaviour was compared with a sample kindly provided by Prof. E. I. Lukyanets.⁸ The present salt-like species $[(\text{CH}_3)_8\text{LZn}](\text{I})_8$ and $[(\text{PtCl}_2)(\text{CH}_3)_6\text{LZn}](\text{I})_6$ were prepared as previously reported.^{9,1a}

Physical Measurements. UV-visible solution spectra were recorded with a Varian Cary 50 Scan spectrometer by using 1-cm quartz cuvettes. Elemental analyses for C, H, and N were provided by the “Servizio di Microanalisi” at the Dipartimento di Chimica, Università “Sapienza” (Rome) on an EA 1110 CHNS-O instrument. The ICP-PLASMA analysis of Al, Na and S was performed on a Varian Vista MPX CCD simultaneous ICP-OES.

Singlet Oxygen Photoproduction. Measurements on the efficacy of $[(\text{CH}_3)_8\text{LZn}]^{8+}$ and $[(\text{PtCl}_2)(\text{CH}_3)_6\text{LZn}]^{6+}$ in the production of $^1\text{O}_2$ were performed in aqueous solution using $\text{PcAlS}_{\text{mix}}$ as reference standard (Pc: phthalocyaninato dianion, $[\text{C}_{32}\text{H}_{16}\text{N}_8]^{2-}$). The alternative use of the Zn^{II} analog, $\text{PcZnS}_{\text{mix}}$, as reference standard was discouraged by the fact that it might show^{3c} a higher degree of aggregation in water solution, as was directly verified by us. $\text{PcAlS}_{\text{mix}}$ is a mixture of compounds with different sulfonation degree and different isomers having formula $\text{PcAlOH}(\text{SO}_3\text{Na})_n$ with $\langle n \rangle \sim 3$. As reported,¹⁰ $\text{PcAlS}_{\text{mix}}$ was prepared by us from PcAlCl as follows:

PcAlCl (210 mg; dye content ~85%) was mixed with oleum (1.6 mL containing 20% SO_3) and the mixture was heated at 110 °C under stirring for 30'. After cooling, the mixture was poured on ground ice (~20 g), brought to neutrality by a solution of NaOH (colour change from green to blue). After evaporation of solvent in air, the solid residue was kept under vacuum and then Soxhlet extracted with methanol for 12 h. After cooling and centrifugation, the solution was evaporated in air and the solid residue was dried under vacuum (192 mg, yield 50%). Calcd for the formula $\text{PcAlOH}(\text{SO}_3\text{Na})_{3.8} \cdot 16\text{H}_2\text{O}$: C, 31.18; H, 3.70; Al, 2.19; N, 9.09; Na, 7.09; S, 9.88%. Found: C, 30.62; H, 3.17; Al, 1.98; N, 8.80; Na, 6.77; S, 9.82%. UV-visible spectral data in H_2O are listed in Table 1. A sample of $\text{PcAlS}_{\text{mix}}$ with $\langle n \rangle \sim 3$, received kindly by Prof. E. A. Lukyanets (University of Moscow) showed identical UV-visible spectra and photochemical efficacy in the production of singlet oxygen. These findings confirm that small differences of sulfonation degree and sample composition do not affect the spectral properties and the singlet oxygen quantum yield

(Φ_{Δ}) of the mixture.¹¹ Both our and Lukyanets' samples were used in this work as reference standards.

The efficacy as photosensitizers of the two cations $[(\text{CH}_3)_8\text{LZn}]^{8+}$ and $[(\text{PtCl}_2)(\text{CH}_3)_6\text{LZn}]^{6+}$ in the production of $^1\text{O}_2$ was examined by analysing the decomposition of the scavenger ADMA (tetrasodium-9,10-anthracenediyl-bis(methylene)malonate), obtained from the corresponding acid salted with NaOH up to pH \sim 7.0) which has been suggested as a specific and very reactive probe for $^1\text{O}_2$ detection in aqueous media.^{11,12} A profile of the procedure used for the studied species, including PcAIS_{mix}, is as follows.

A water solution (2.00 mL; pH = 6.5-7.0) of the monomeric photosensitizer ($c \sim 4 \cdot 10^{-6}$ M; absorbance \sim 0.4 at the wavelength of irradiation) containing the anionic surfactant SDS ($\text{H}_2\text{O}/\text{SDS}$; $[\text{SDS}] = 0.020$ M; as to the role of SDS see the later discussion) and the scavenger ADMA ($c \sim 1 \cdot 10^{-4}$ M) was irradiated in a 1.00 cm-quartz cell by a laser source (Premier LC Lasers/HG Lens, Global Laser) in the region of the Q band ($\lambda_{\text{irr}} = 670$ nm). Illumination was directed normally both to the surface of the solution and to the spectrophotometric radiation. During the experiment, continuous magnetic stirring ensured homogeneity of the solution while a circulating water system kept the temperature constant at 30°C. The power of irradiation (W), accurately measured by a radiometer (ILT 1400A/SEL100/F/QNDS2, International Light Technologies), was fixed at ca. 5 mW. For each experiment the pH of the solution was measured before and after irradiation and no changes of its value (range 6.5 - 7.0) were observed.

The decay of trap's absorption at 380 nm was monitored as a function of the time, and sensitizer stability was also checked under irradiation. Because of the fast decay of $^1\text{O}_2$ in aqueous solution, the photo-oxidation of the scavenger ADMA, under the experimental conditions described above, follows a first-order kinetic equation.¹³ The relative photosensitizing activity of the present Zn^{II} and $\text{Zn}^{\text{II}}/\text{Pt}^{\text{II}}$ cationic species in the production of singlet oxygen with respect to the reference PcAIS_{mix} was determined on the basis of the following equation:

$$\text{Relative photosensitizing activity} = \frac{k_I W_{abs}^R}{k_I^R W_{abs}} \quad (1)$$

where k_I and k_I^R are the ADMA bleaching first-order rate constants of octa- or the hexacation and the reference PcAIS_{mix}, respectively; W_{abs} and W_{abs}^R are the rate of light absorption by the

examined cation and the reference, respectively, calculated considering an optical path length of 2.1 cm (total volume of solution and magnet in the cuvette = 2.1 mL; $W_{abs} = W (1-10^{-2.1A})$).¹⁴

Fluorescence measurements. Fluorescence measurements for the present multicationic species were performed in water solution containing 0.020 M SDS using a Cary Eclipse-Varian spectrofluorometer and a 1-cm quartz cell. The fluorescence quantum yields (Φ_F) of the Zn^{II} and Zn^{II}/Pt^{II} cations were determined by a comparative method with chlorophyll-*a* as the reference standard ($\Phi_F = 0.32$, ether solution), according to the following equation:

$$\Phi_F^S = \frac{G^S * n_{H2O}^2 * A^R}{G^R * n_{ether}^2 * A^S} \Phi_f^R \quad (2)$$

where G is the integrated emission area, n is the refractive index of the solvent, A is the absorbance at the excitation wavelength, and S and R indicate the sample (octa- or hexacation) and the reference. The addition of SDS 0.020 M does not change the refractive index of water in a significant way.¹⁵ In all cases the absorbance of the solution was below 0.1 at and above the excitation wavelength ($\lambda_{exc} = 600$ nm).

Cell lines and treatments. All chemicals used for this type of experiments on the two cations $[(CH_3)_8LZn]^{8+}$ and $[(PtCl_2)(CH_3)_6LZn]^{6+}$ and on PcAlS_{mix} were from Sigma unless otherwise specified. The melanoma C8161 and oral squamous carcinoma CA-1 cell lines were a kind gift of Prof. Mike Philpott and Prof. Ian McKenzie, Queen Mary University, London. They were cultured in Roswell Park Memorial Institute (RPMI) medium supplemented with 10% fetal bovine serum (FBS) and Rheinwald's medium (RM+) (Dulbecco's modified Eagle's medium-F12 (DMEM/F12)) with supplements, respectively.¹⁶

For the **irradiation dose response** experiment, cells were seeded at a density of 10^4 cells/cm² in 12-well plates and treated 24 hours later with $5.0 \cdot 10^{-7}$ M of complexes in medium, following which cells were allowed to incubate for 5 hours. The medium was then replaced with fresh medium and the cells were irradiated with red light (120 LED 660 nm handheld unit, The LED Man, USA), centered at 660 nm (spectral line full width at half-maximum, $\Delta\lambda = 20$ nm) and 50 mW/cm² radiant power for a range time from 0 to 900 seconds (0 to 45 J/cm²). The upper limit of this range (45 J/cm²) was then selected as the light dose for all further experiments.

For the *complex stability* experiment, solutions of each complex ($1.0 \cdot 10^{-6}$ M) were prepared in 12-well plates and irradiated with red light (900 s, 45 J/cm^2) after which medium was recovered and analyzed by spectrophotometry.

For *cell viability*, cells were treated as for the irradiation dose response experiments above with various complex concentrations (0-250 nM for the octa- and hexacations, 0-500 nM for PcAIS_{mix}), and after 5 hours the medium was replaced with fresh one just prior to irradiation (900 s, 45 J/cm^2). After 24 hours of incubation, cells were supplemented with 10% Alamar Blue® (ABD Serotec) reagent dissolved in culture medium and further incubated for 2.5 hours, at the end of which period supernatants were read for fluorescence in a plate reader (excitation 530 nm, emission 590 nm).

For *apoptosis measurement*, cells were treated as above specified with $1.0 \cdot 10^{-7}$ M complex, irradiated with red light (900 s, 45 J/cm^2) and after the 24 hour incubation period, the cells were detached from the wells with 0.025% trypsin/PBS (Thermo Fisher, UK). Cells were then resuspended in 150 μL growth medium, added with 150 μL of Guava Nexin reagent (Millipore Inc) and incubated in the dark for 20 min prior to analysis on a Muse flow cytometry machine (Millipore Inc).

For the *cell uptake* experiment, cells were treated as indicated above with $1.0 \cdot 10^{-6}$ M complexes and, after the initial 5 hours of incubation, the wells were rinsed twice with phosphate buffered saline (PBS) and lysed in RIPA buffer (10 mM Tris-Cl (pH 8.0, 1 mM EDTA, 1% Triton X-100, 0.1% sodium deoxycholate, 0.1% SDS, 140 mM NaCl)). Lysates were clarified by centrifugation and examined by emission fluorescence (360 nm excitation, 680-685 nm emission) using a Fluoro MAX 3 fluorimeter (Horiba). Standard solutions of each complex were used for calibration. Total protein content of the lysates was carried out by the DC Protein Assay (BioRad Laboratories, Inc) according to manufacturer's protocol.

For *cell cycle analysis*, cells were treated as for the apoptosis measurement experiment until the irradiation step (900 s, 45 J/cm^2) after which they were incubated for a further 2 hours at 37°C and then collected with 0.025% trypsin/PBS, spun at 300 rpm for 10 min and fixed in 70% ethanol/water at 4°C overnight. Cells were then centrifuged again and resuspended in Propidium Iodide/RNase solution (10 mM sodium phosphate, 137 mM NaCl, 2.7 mM KCl, 40 $\mu\text{g/mL}$

propidium iodide, 100 $\mu\text{g}/\text{mL}$ RNase A, pH 7). Following a 2 hour incubation at room temperature, cells were analysed on a BD LSR II flow cytometer (BD Biosciences).

Results and Discussion

UV-visible Spectra in non Aqueous Solvents, H_2O and $\text{H}_2\text{O}/\text{SDS}$ Solutions

The cations $[(\text{CH}_3)_8\text{LZn}]^{8+}$ and $[(\text{PtCl}_2)(\text{CH}_3)_6\text{LZn}]^{6+}$ (Scheme 1) exhibit in non aqueous low-donor solvents (pyridine, DMSO, DMF) a UV-visible spectrum characterized by a narrow and sharp Q band (peak maximum in the range 665-670 nm), in line with expectation for a monomeric species.^{1a,9} Both charged species (as iodide salts) exhibit moderate solubility in H_2O , in which they show two intense absorptions in the Q-band region (Figure 2), with maxima of comparable intensity at 625 and 655 nm, attributable, as was widely illustrated,^{6,9} to the presence of a dimer-monomer equilibrium, with the peak at lower energy (655 nm) assigned to the monomeric species. As also shown in Figure 1, addition of SDS (0.020 M, Critical Micelle Concentration, $\text{CMC} = 8.2 \cdot 10^{-3}$ M) to the aqueous solutions of the two charged macrocycles determines the shift of the dimer-monomer equilibrium completely towards the formation of the monomer (sharp Q-band maximum at 661 nm), supposedly due to association of both macrocycles to the negatively charged micelle surface. As the absorption spectrum of the monomeric species is crucial to estimate the $^1\text{O}_2$ photoproduction of the sensitizer (dimeric forms are not photoactive),^{2d,3c,7} all the experiments were conducted after addition of SDS 0.020 M and complete monomerization of the complex (24 h). Addition of the surfactant SDS 0.020 M to a water solution of the reference $\text{PcAlS}_{\text{mix}}$ does not cause any noticeable change in shape and intensity of the spectra, which confirms that $\text{PcAlS}_{\text{mix}}$ is present in H_2O in its monomeric form. Table 1 shows the UV-visible spectral data of the present species in aqueous solution.

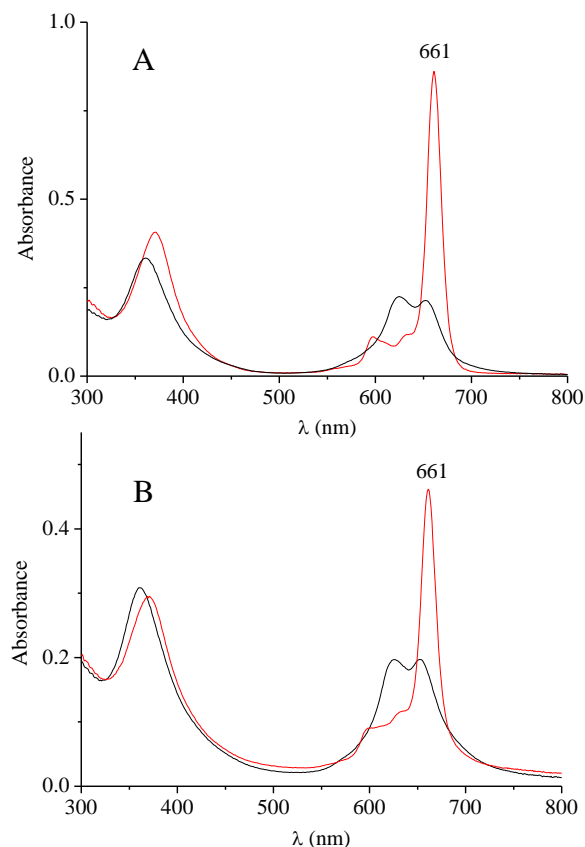


Figure 1. A) UV-visible spectra in water solution of A) $[(\text{CH}_3)_8\text{LZn}]^{8+}$ ($c = 4.6 \times 10^{-6}$ M) and B) $[(\text{PtCl}_2)(\text{CH}_3)_6\text{LZn}]^{6+}$ ($c = 3.3 \cdot 10^{-6}$ M) before (black line) and after (red line) addition of 0.020 M SDS (CMC = $8.2 \cdot 10^{-3}$ M).

Table 1. UV-visible Spectral Data (λ , nm) of $[(\text{CH}_3)_8\text{LZn}]^{8+}$, $[(\text{PtCl}_2)(\text{CH}_3)_6\text{LZn}]^{6+}$ and $\text{PcAlS}_{\text{mix}}$ in H_2O and $\text{H}_2\text{O}/\text{SDS}$.

	Solvent	Soret-band region			Q-band region	Ref. ^a
		λ , nm ($\log \epsilon$)				
$[(\text{CH}_3)_8\text{LZn}]^{8+}$	H_2O^b	360 (4.89)	626 (4.49)	654 (4.70)	9	
	$\text{H}_2\text{O}/\text{SDS}$	372 (4.94)	597 (4.35)	661 (5.27) ^c	tw	
$[(\text{PtCl}_2)(\text{CH}_3)_6\text{LZn}]^{6+}$	H_2O^d	360 (4.82)	625 (4.64)	650 (4.59)	17	
	$\text{H}_2\text{O}/\text{SDS}$			661 (5.15)	6	
$\text{PcAlS}_{\text{mix}}$	H_2O	351 (4.91)	609 (4.55)	678 (5.27)	tw	

^atw = this work; ^b $\log \epsilon$ values obtained at $c = 5.18 \cdot 10^{-7}$ M; ^c a $\log \epsilon$ value of 5.32 at 661 nm was previously reported.⁶; ^d $\log \epsilon$ values obtained at $c = 5.0 \cdot 10^{-5}$ M.

Singlet Oxygen Production in Water Solution

The experiments on the photosensitizing activity for the generation of singlet oxygen, $^1\text{O}_2$, of the cations $[(\text{CH}_3)_8\text{LZn}]^{8+}$ and $[(\text{PtCl}_2)(\text{CH}_3)_6\text{LZn}]^{6+}$ were performed in $\text{H}_2\text{O}/\text{SDS}$ solution, where

as above noticed, they are present fully in their monomeric form. The photochemical study was carried out by the comparative method described in the Experimental Section, with ADMA used as the scavenger. The photodynamic potential was evaluated by comparing the ADMA bleaching first-order rate constants obtained for each one of the two species with that of the standard PcAIS_{mix} determined under the same experimental conditions ([SDS] = 0.020 M). PcAIS_{mix} is a well-known singlet oxygen sensitizer, commercially known as Photosens[®] presently in clinical use in Russia; it is monomeric in water solution and gives reproducible experiments and, on this basis, it can be used for comparison purposes in singlet oxygen quantum yield measurements in H₂O on phthalocyanine or porphyrazine macrocycles.^{11,18}

Figure 2 exemplifies the results of a typical experiment performed on the Zn^{II} octacation [(CH₃)₈LZn]⁸⁺. Figure 2A shows the initial UV-visible spectrum of the solution containing the sensitizer (blue line, Q band at 661 nm) and the peaks of ADMA in the region 300-400 nm superimposed with the Soret band of the complex. Irradiation of the solution causes a complete disappearance of the ADMA peaks within 10 minutes, leaving the spectrum of the Zn^{II} complex unmodified. Figure 2B shows the ADMA-absorbance time decay at 380 nm which can be fitted according to a first-order law, thus allowing determination of the related *k* value. As can be seen, the absorbance of the Q band of the sensitizer, also checked during irradiation, remains constant during the experiment, indicating that the sensitizer is not undergoing photobleaching at all. The *k* values measured for coupled experiments, conducted strictly under the same experimental conditions on the Zn^{II} (or Zn^{II}/Pt^{II}) species and the reference PcAIS_{mix} were used in equation 1 reported in the Experimental Section to evaluate the relative photosensitizing activity of the studied cationic species.

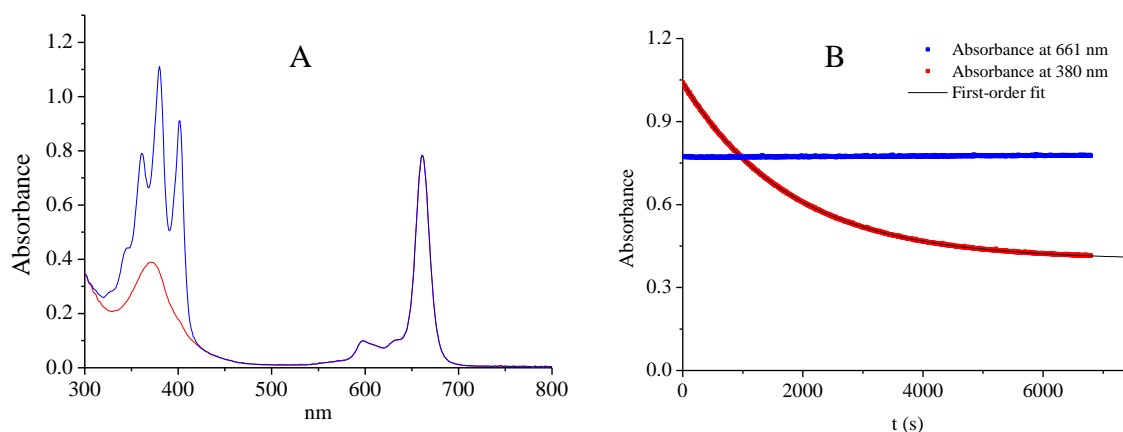


Figure 2. A) UV-visible spectra of $[(\text{CH}_3)_8\text{LZn}]^{8+}$ and ADMA in $\text{H}_2\text{O}+\text{SDS}$ ($[\text{SDS}] = 0.020 \text{ M}$) before (blue line) and after (red line) laser irradiation; B) Absorbance values indicating ADMA photo-oxidation (red plot) and sensitizer Q-band maximum (blue dots) during irradiation; the related first-order exponential fit (black line) is also shown.

The Φ_{Δ} values of $\text{PcAIS}_{\text{mix}}$ reported in the literature fall in the range $(0.34 \div 0.42) \pm 0.06^{19}$ and refer to different experimental conditions (in terms of medium composition, surfactant, irradiation range) than those required for the present comparative study. For this reason and in the attempt to evaluate properly the photosensitizing efficacy in $^1\text{O}_2$ production of the monomeric Zn^{II} and $\text{Zn}^{\text{II}}/\text{Pt}^{\text{II}}$ complexes in water solution, it was considered more reliable to express their activity as “*relative photosensitizing activity*” compared to that shown by the reference standard $\text{PcAIS}_{\text{mix}}$ under strictly identical experimental conditions (H_2O , $[\text{SDS}] = 0.020 \text{ M}$, $\lambda_{\text{irr}} = 670 \text{ nm}$).

Table 2 lists the *relative photosensitizing activity* values for $^1\text{O}_2$ production and also the fluorescence quantum yields (Φ_{F}) measured for the present two cationic complexes in $\text{H}_2\text{O}/\text{SDS}$ solutions. Noticeably, experimental data clearly indicate that both cationic species in their monomeric form exhibit an efficiency for the production of $^1\text{O}_2$ in water solution 2.3-2.5 times higher than that of the reference standard $\text{PcAIS}_{\text{mix}}$ arbitrarily fixed as 1. Thus, these data clearly propose the two multicharged cations $[(\text{CH}_3)_8\text{LZn}]^{8+}$ and $[(\text{PtCl}_2)(\text{CH}_3)_6\text{LZn}]^{6+}$ as highly promising photosensitizers in PDT, deserving special attention in the context of the literature data reported on water soluble porphyrazine and phthalocyanine macrocyclic species.^{3b,c,18,20} Accordingly, the observed Φ_{F} values obtained for the same cationic complexes are lower than that of $\text{PcAIS}_{\text{mix}}$, in line with expectation.

Table 2. Photophysical and Photochemical Data for $[(\text{CH}_3)_8\text{LZn}]^{8+}$, $[(\text{PtCl}_2)(\text{CH}_3)_6\text{LZn}]^{6+}$, and $\text{PcAIS}_{\text{mix}}$ in $\text{H}_2\text{O}/\text{SDS}$.

Photosensitizer	Solvent	Singlet Oxygen Production ($\lambda_{\text{irr}} = 670 \text{ nm}$)		Fluorescence Emission ($\lambda_{\text{exc}} = 600 \text{ nm}$)	
		λ_{max} (nm)	Relative photoactivity ^a	λ_{em} (nm)	Φ_{F} ^a
$[(\text{CH}_3)_8\text{LZn}]^{8+}$	$\text{H}_2\text{O}/\text{SDS}$	661	2.5	666	0.23
$[(\text{PtCl}_2)(\text{CH}_3)_6\text{LZn}]^{6+}$	$\text{H}_2\text{O}/\text{SDS}$	661	2.3	666	0.15
$\text{PcAIS}_{\text{mix}}$ ^b	$\text{H}_2\text{O}/\text{SDS}$	678	1	683	0.31

^a Mean value of at least three measurements.

^b The singlet oxygen quantum yield for $\text{PcAIS}_{\text{mix}}$ in phosphate buffer has been reported to be in the range $(0.34 \div 0.42) \pm 0.06$.¹⁹

General Behaviour of the Photosensitizers in Culture Medium

Based on the just described results obtained in water solution on the two multicharged species and aware that dynamics of a sensitizer may be different moving to a biological environment,²¹ further *in vitro* studies were planned. Solutions of the octacation, $[(\text{CH}_3)_8\text{LZn}]^{8+}$, hexacation, $[(\text{PtCl}_2)(\text{CH}_3)_6\text{LZn}]^{6+}$ and the standard reference compound, $\text{PcAIS}_{\text{mix}}$, at $1.0 \cdot 10^{-6} \text{ M}$ concentration were prepared in RPMI media/10% FBS used for cellular culture and their UV-visible spectra were run to ascertain the influence of the medium on the species. Subsequently, spectra were also taken of the species in medium upon irradiation for 900 s ($45 \text{ J}/\text{cm}^2$) with red light under the same experimental conditions as the cell viability experiments, to determine stability of the complexes. The spectra observed for the two cationic species in the region 550-700 nm (Figure 3-A,B) closely recall those reported in the same region in pure water (Figure 1-A,B), displaying two peaks at 625 and 654 nm reflecting a similar monomer/dimer equilibrium for the cationic species as the peaks simplify to a single one following SDS supplementation (data not shown). The wavelength chosen for the irradiation (660 nm) is close to the position of the Q-band maxima for the photoactive monomeric forms of both cationic species. Taking into account the emission spectrum of the 660 nm LED source and the water solution absorption spectra of the monomeric $[(\text{CH}_3)_8\text{LZn}]^{8+}$, $[(\text{PtCl}_2)(\text{CH}_3)_6\text{LZn}]^{6+}$ and $\text{PcAIS}_{\text{mix}}$, it was resulted that all the compared species were investigated under similar irradiation conditions.

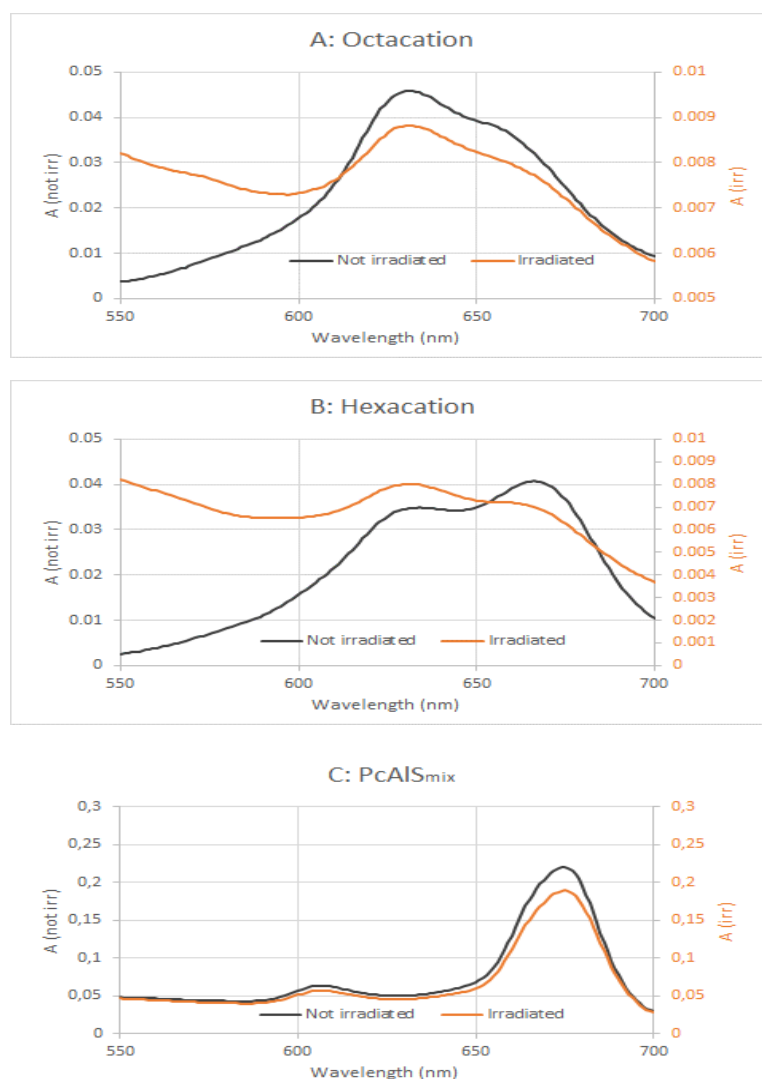


Figure 3. Absorption spectra in culture medium of the two cationic species (A,B) and the reference PcAIS_{mix} (C) before (not irr, black) and after (irr, orange) irradiation with red light (900 s, 45 J/cm²).

As can be seen in Figure 3-A,B, irradiation with red light dramatically reduces the concentration of both cationic photosensitizers (see right Y axis) reasonably by photobleaching, which is practically absent for PcAIS_{mix} (Figure 3-C). It is instead observed that irradiation of the octacation minimally influences the ratio between the monomer and the aggregated form (Figure 3-A), whereas a small change of the relative intensity of the Q-band maxima of the type dimer → monomer is observed for the hexacation (Figure 3-B).

Irradiation dose response of complex treated cells. The effect of increasing doses of light irradiation (0 → 900 s or 0 → 45 J/cm²) was investigated on both cell lines (C8161 and CA-1) at a constant complex concentration of 5.0·10⁻⁷ M, and it is reported in Figure 4. The dose light of 45

J/cm² was selected as the dose to use in all cellular experiments, as it maximizes the observable phototoxicity while still exerting negligible effects on untreated cells.

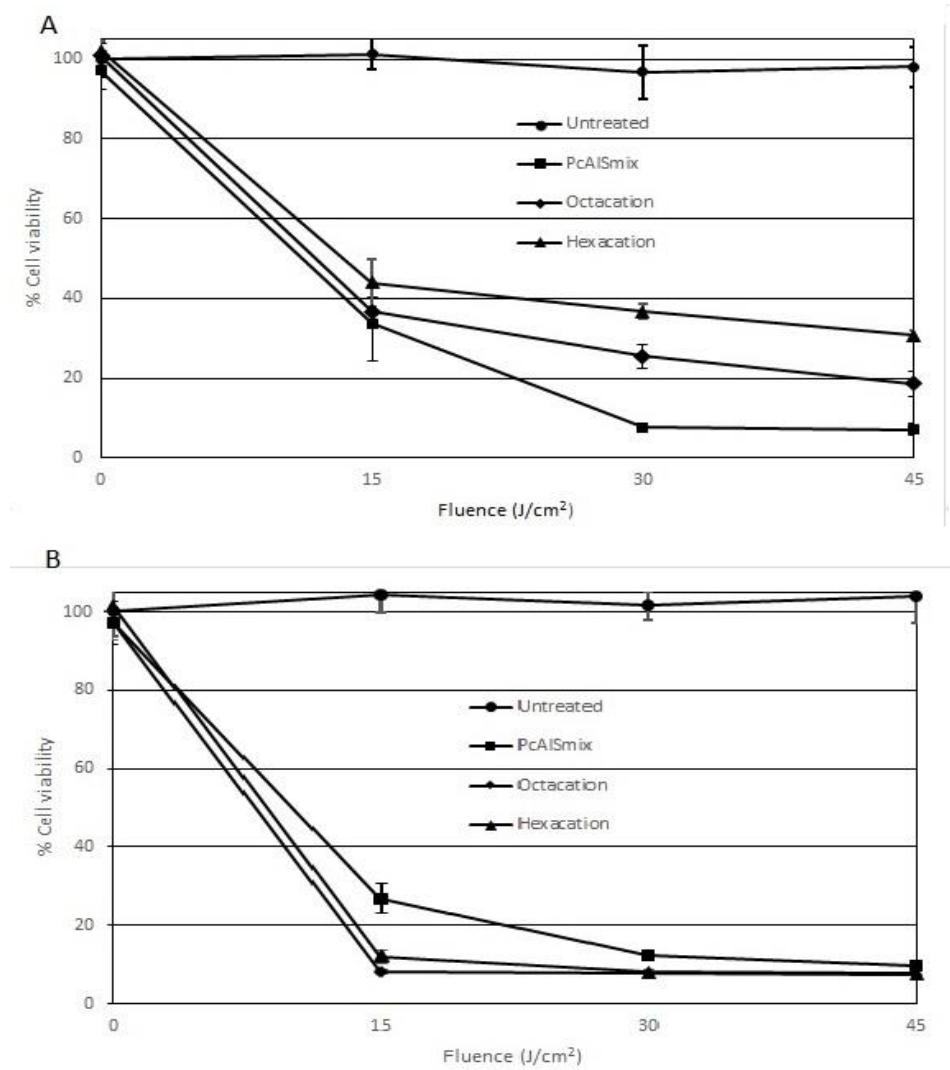


Figure 4. Irradiation dose response of cell viability in C8161 (A) and CA-1 (B) cells for the three macrocycles at $5 \cdot 10^{-7}$ M concentration and untreated control. Data are the average values of N = 3 experiments.

Cellular uptake. The cellular uptake of the complexes was measured to assess whether the different charge of the molecules would result in differential cellular penetration. Quantification via fluorescence of cell lysates normalized to protein content for C8161 cell line (Figure 5), shows indeed a much higher (around 10-fold) uptake of the two cationic species with respect to PcAlS_{mix}. Similar results were also found for the CA-1 cell line. This points to a higher cell permeation of the

cationic complexes which is in line with the established understanding that a positive charge on a molecule facilitates its penetration of the negatively charged cell membrane and also with the observation that sulfonation impedes cellular penetration of PcAIS_{mix}.²²

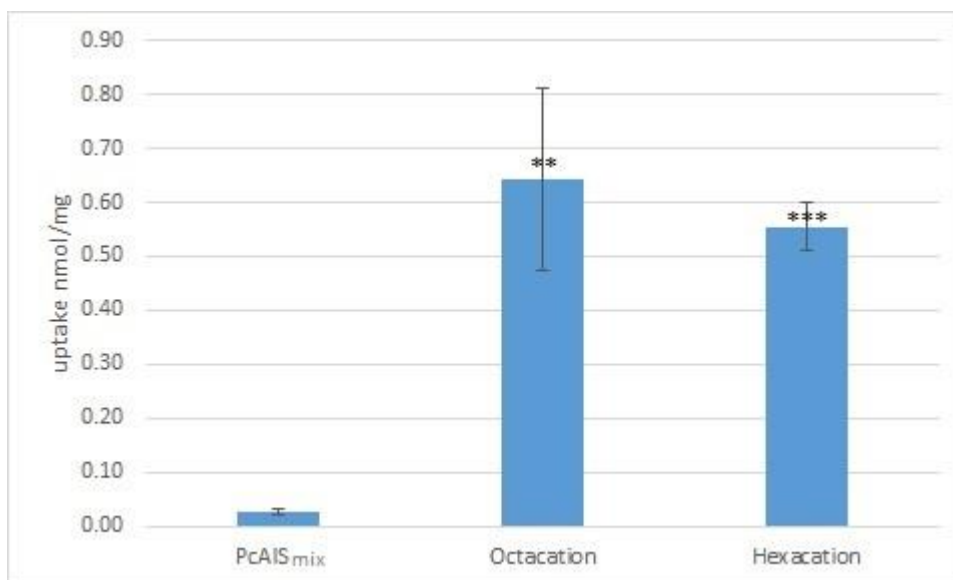


Figure 5. Cellular uptake values for the three macrocycles in C8161 cells. Data are the average values of N = 3 experiments. (** p<0.01; *** p<0.001)

Cell viability following treatment with complexes and irradiation. Both cell lines (C8161 and CA-1) were treated with $[(\text{CH}_3)_8\text{LZn}]^{8+}$, $[(\text{PtCl}_2)(\text{CH}_3)_6\text{LZn}]^{6+}$ (0 to 250 nM) and PcAIS_{mix} (0 to 500 nM), incubated for 5 hours and irradiated with red light (660 nm) for 900 s (45 J/cm²) as determined earlier. Viability results as measured by the Alamar Blue assay (N = 3 replicates) and fitted to a standard Hill dose-response curve, showed no significant toxicity of any of the examined species in the absence of red light irradiation within the concentration ranges used as shown in Figure 6 (black line). This Figure and Table 3 report the half-maximum inhibitory concentration (IC₅₀) values for the complexes under irradiation which are significantly different for the examined species, with values in the order octacation < hexacation < reference PcAIS_{mix}. It is apparent that, in spite of their generally lower IC₅₀ values, the cationic photosensitizers have a lower maximal toxicity (20-30% residual viability) than PcAIS_{mix} (10-15%). The reasons for this

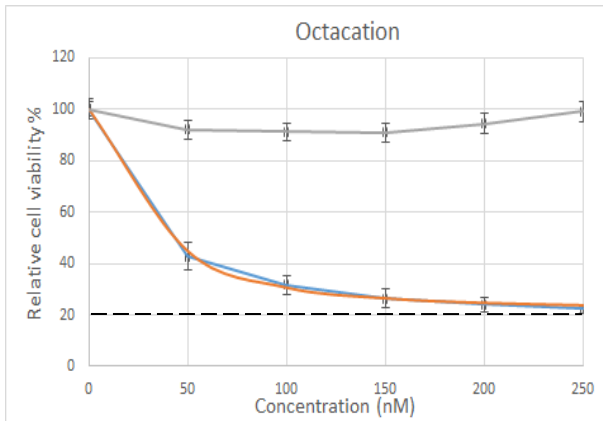
are presently unclear but may point to the existence of subpopulations of cells somehow resistant to the effects of the compounds. It would be interesting to determine the biological basis of this phenomenon.

Noteworthy, the IC₅₀ absolute values are in general lower for the C8161 than for CA-1 highlighting a lower sensitivity of keratinocytes to this photodynamic treatment. In conclusion, these viability data identify the octacation as the most active photosensitizer among the examined species.

Table 3. Best fit of IC₅₀ values (nM) for [(CH₃)₈LZn]⁸⁺, [(PtCl₂)(CH₃)₆LZn]⁶⁺ and PcAlS_{mix} for the two cell lines. Data average and standard deviation on N = 3 experiments (* p<0.05; ** p<0.01; *** p<0.001)

Sensitizer	IC ₅₀ (C8161)	IC ₅₀ (CA-1)
[(CH ₃) ₈ LZn] ⁸⁺	30 ± 10**	55 ± 8***
[(PtCl ₂)(CH ₃) ₆ LZn] ⁶⁺	75 ± 7*	105 ± 3*
PcAlS _{mix}	100 ± 18	130 ± 12

A



B

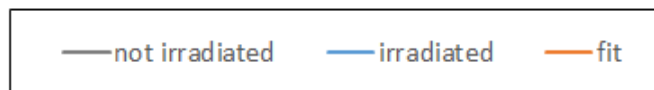
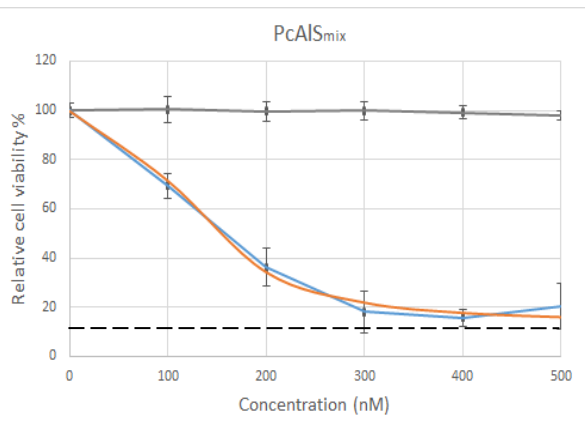
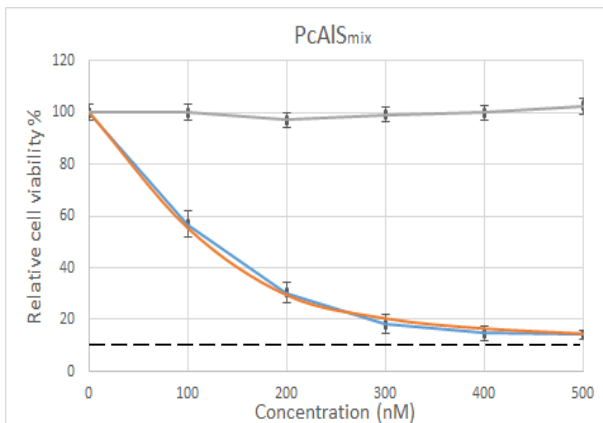
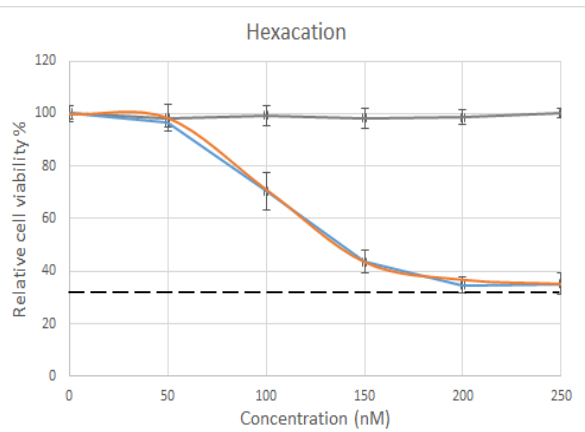
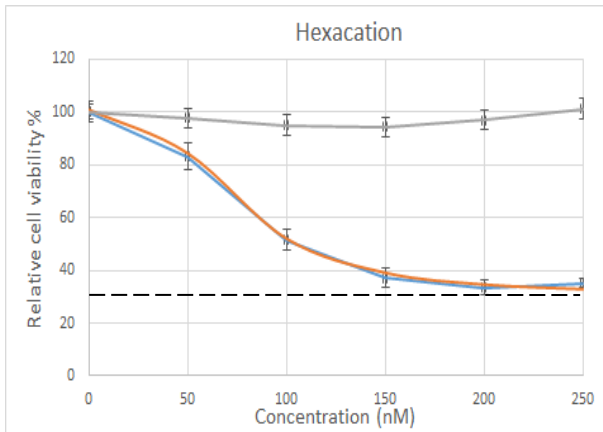
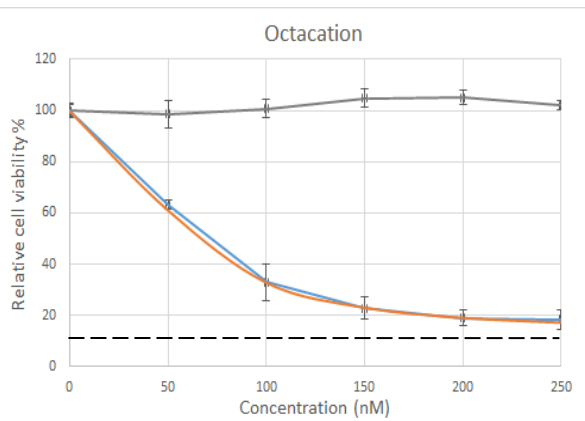
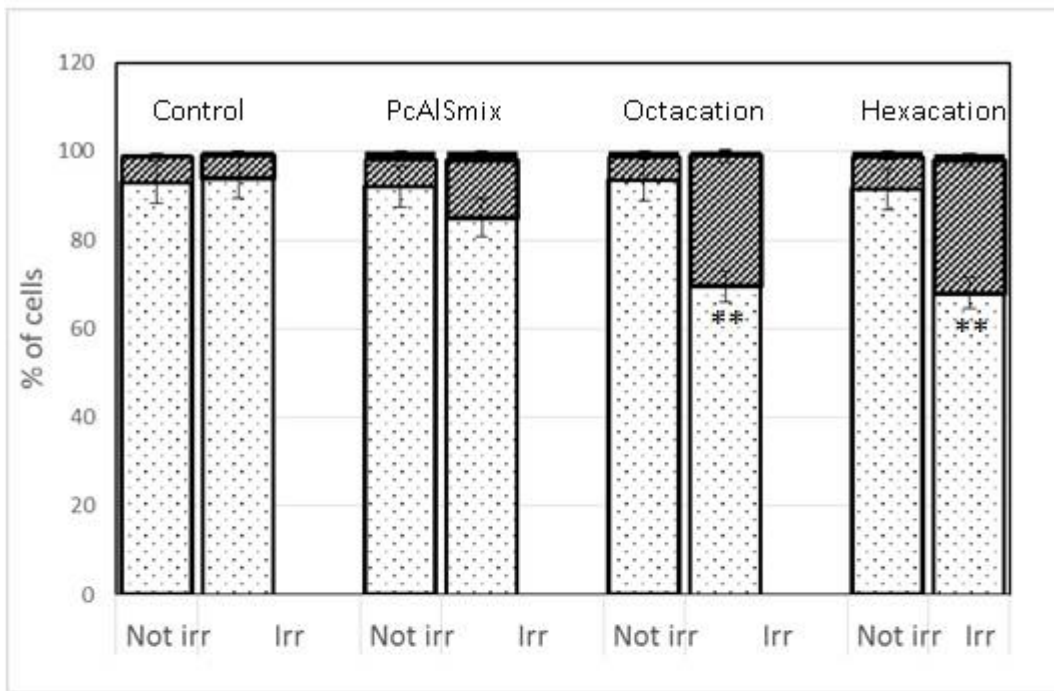


Figure 6. Cellular viability experiments on cells treated with the indicated concentrations of complexes and irradiated (45 J/cm^2). A, C8161 cells; B, CA-1 cells. Dashed horizontal lines indicate maximal effect.

Cellular death modality. Cell death in general and PDT induced cell death in particular may happen via one of two main pathways: organized cell death (apoptosis) or disordered death (necrosis). Apoptosis has the potential clinical advantage of not causing inflammation, one of the known drawbacks of photodynamic therapy in general.²³ The pathway to cellular death (apoptosis or necrosis) induced by the examined cationic species and PcAIS_{mix} was therefore investigated by the Annexin V protocol, a simple and fast method which quantifies apoptosis indirectly via the amount of phosphatidylserine present on the outer side of cell membranes which correlates to apoptosis. This is labelled by the protein Annexin V and read by flow cytometry. As shown in Figure 7 flow cytometry analysis of the cell viability status in C8161 (A) and CA-1 (B) suggests that apoptosis is the main cellular death pathway for the all examined species, even those with a higher phototoxicity as the octa- and hexacations. This result supports the two cationic species as promising molecules for medical use in anticancer therapy.

A



B

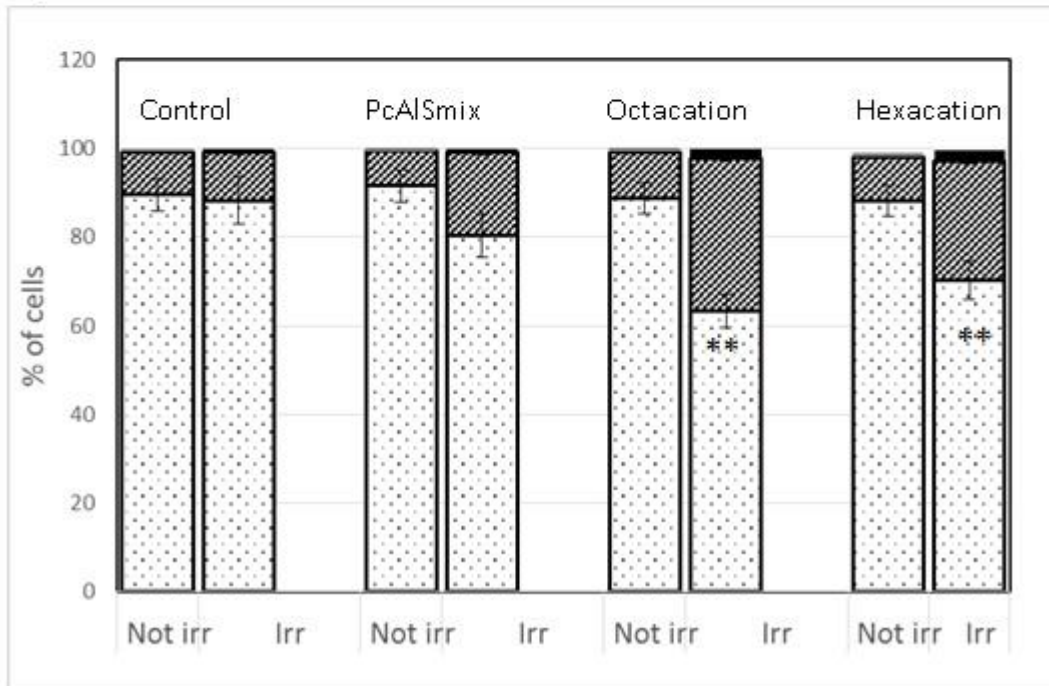


Figure 7. Flow cytometry analysis of cell viability status in C8161 (A) and CA-1 (B) cells for the three macrocycles (100 nM) without (not irr) and with (irr) light irradiation. Data shown are the average values of N = 3 experiments. (** p<0.01)

Cell cycle distribution investigation. To complete this preliminary investigation on the cellular effect of the investigated species, we decided to study the cell cycle distribution of the cells under study following drug treatment and light irradiation by means of propidium iodide (PI) flow cytometry. PI is a highly fluorescent nucleic acid specific stain imparting fluorescence to each cell in an amount proportional to its DNA content. Because all viable and resting (G1 phase) human diploid cells contain 46 chromosomes, their PI fluorescence is roughly the same. As a cell replicates its chromosome count gradually increases (S phase) up to 92 (G2 phase), only to return to 46 once the cell physically divides. Dying cells instead degrade their DNA, display a PI fluorescence below that of the G1 phase and are therefore labelled sub-G1. Thus, the PI fluorescence distribution of cells gives an indication of how many cells are undergoing each of the cell phases at any given time and how many are non viable and this in turn supplies information on any perturbations of the normal cycle, such as cell cycle arrests, due to cellular damage. Figure 8-A shows an example distribution of PI fluorescence on untreated (healthy) cells. Panels B and C quantify the same distribution of variously treated cells in each phase, grouping S and G2 phase cells together for clarity. Results on both cell lines show that whereas the octacation complex $[(\text{CH}_3)_8\text{LZn}]^{8+}$ simply causes an increase in the sub-G1 (dead cell) fraction, PcAIS_{mix} increases the fraction of cells in S/G2 cell cycle (implying S phase arrest) of cells. This could be an indication of an altogether different death pathway provoked by the two species with PcAIS_{mix} interfering with the DNA replication event and the octacation perhaps targeting other cell machinery components. The hexacation does not seem to induce a particular disruption of the cell cycle distribution except for a minor increase in G1 phase cells in the CA-1 line. It would be interesting to confirm this and verify whether the complex is able to localize in the nucleus and interact with DNA *in vitro* as it was shown to do in solution as platinated alkylating drugs are associated with G1 phase arrest.

The data obtained in the present *in vitro* experiments point first of all to a better quantitative performance of the cationic complexes on the two cancer cell lines tested compared to the PcAIS_{mix} control. This result is in spite of the lower observed stability of these complexes to irradiation in culture medium and can be attributed partly to their higher extent of cellular incorporation and partly to their higher photosensitizing activity for the production of singlet

oxygen in aqueous environment. The complexes elicit a higher amount of apoptotic cell death compared to the reference standard and appear to act along a different mechanism.

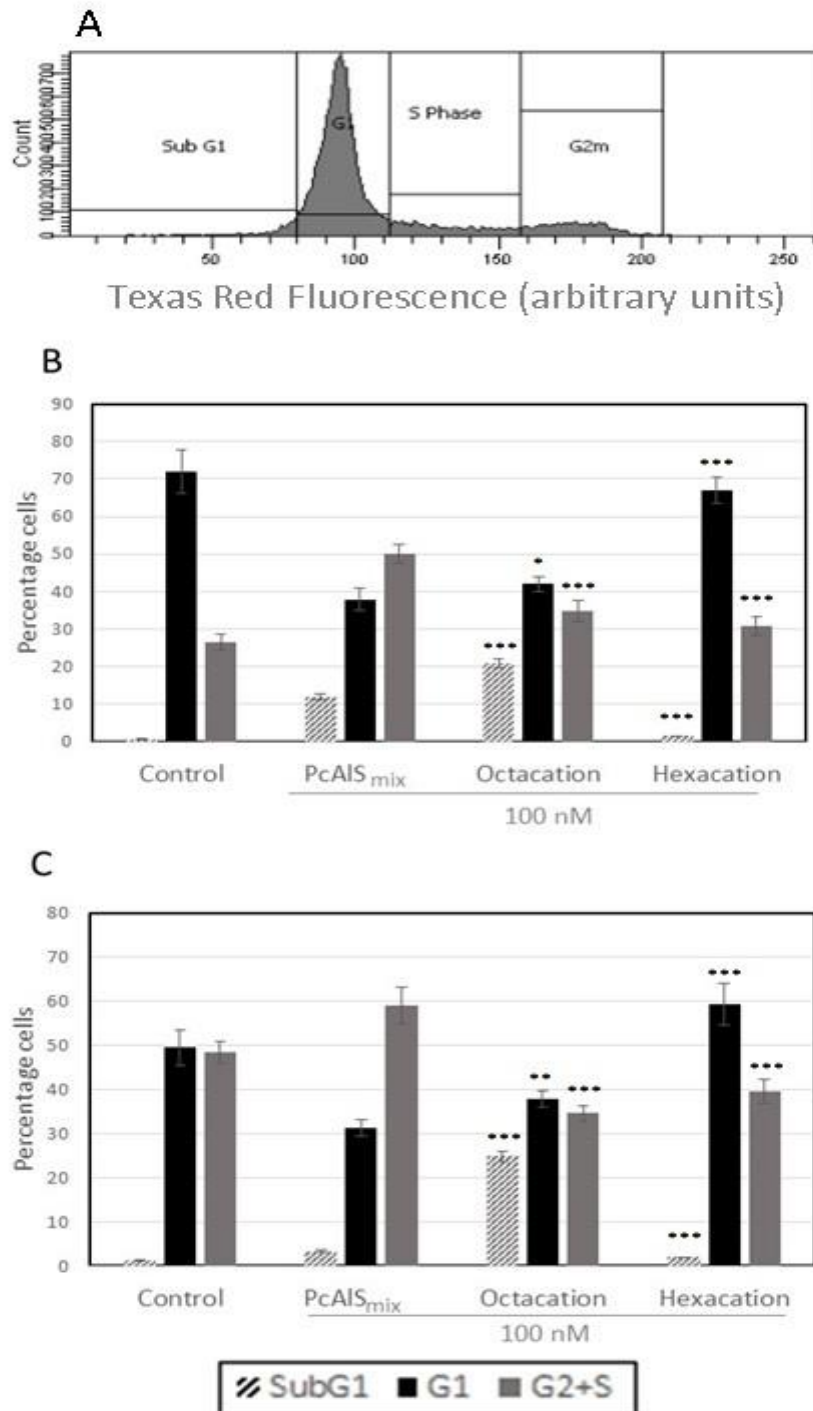


Figure 8. Cell cycle flow cytometry results. A, sample instrumental plots for untreated normal C8161 cells; B, C summary of cell cycle distributions of C8161 and CA-1 cells treated with the three complexes. Data is the average of N = 3 experiments. (* p<0.05; ** p<0.01; *** p<0.001)

Conclusion

As previously verified, the cation $[(\text{CH}_3)_8\text{LZn}]^{8+}$, and the related species $[(\text{PtCl}_2)(\text{CH}_3)_6\text{LZn}]^{6+}$ (both neutralized by I^- ions) behave as excellent photosensitizers in a nonaqueous solvent (DMF), where they are present exclusively in their monomeric form and are able to interact in water solution, although in the presence of aggregation, with a G4 quadruplex telomeric structure and ds-B-DNA, thus evidencing potentialities for multimodal anticancer curative applications. It was believed of great interest to obtain more precise information on the photosensitizing activity of the two porphyrazine positively charged complexes in water solution in the absence of aggregation, and experiments were conducted in water in the presence of SDS. UV-visible spectra in the medium $\text{H}_2\text{O}/\text{SDS}$ indicate that both species, due to interaction with SDS micelles, are present uniquely in their monomeric form. Data available on the relative activity for singlet oxygen production prove that both the octacation and the hexacation have photosensitizing properties 2.3-2.5 times higher than the used reference standard $\text{PcAlS}_{\text{mix}}$ (Photosens[®]). The effects of both cationic species on the cell lines C-8161 (melanoma) and CA-1 (oral squamous cell carcinoma) by *in vitro* tests under appropriate experimental conditions were also examined. Although aggregation is occurring in the culture medium, the total data obtained in the cellular environment clearly indicate that the two cations behave more efficiently than the reference $\text{PcAlS}_{\text{mix}}$ in terms of cellular incorporation, photomediated toxicity, and cell death modality, which is indicative of a largely prevalent apoptosis versus necrosis. As a next step, the intrinsic fluorescence properties highlighted in water solution will allow us to investigate the different subcellular localization of the studied cationic complexes and their overall photochemistry following irradiation *in vitro* will be studied. Moreover, the cellular pathways triggered by photodynamic treatment with the complexes remain to be elucidated, and as a consequence whether these molecules could bring about selective benefits on some particular types of cancer either on their own or in combination with other agents. However, the preliminary observation that both the octacation and the hexacation display enhanced cellular incorporation and higher potency towards highly common (squamous cell carcinoma) and highly malignant (melanoma) skin cancers makes them interesting objects of study as well as potentially promising drugs.

Author Information

Corresponding Authors

*E-mail: mariapia.donzello@uniroma1.it Phone +39 0649913330

*E-mail: elisa.viola@uniroma1.it Phone +39 0649913330

*E-mail: g.trigiane@qmul.ac.uk

Notes

The authors declare no competing financial interest.

ACKNOWLEDGMENT

Financial support by the University of Rome La Sapienza (Progetto di Ricerca di Università - Anno 2014 - prot. C26A14EWLE) is gratefully acknowledged. M.P.D. and E.V. are grateful to the Consorzio Interuniversitario di Ricerca in Chimica dei Metalli nei Sistemi Biologici (CIRCMSB) for scientific support. Thanks are expressed to Prof. Fabrizio Monacelli for helpful discussions. M.P.D. and E.V. are grateful to Maria Luisa Astolfi for ICP-PLASMA analyses. G.T. acknowledges Mr Sreekanth Reddy Vootukuri for his help with the cell biology experiments.

Abbreviations used

ADMA, tetrasodium 9,10-anthracenediyl-bis(methylene)malonate; CMC, Critical Micelle Concentrations; DMEM/F12, Dulbecco's modified Eagle's medium-F12; FBS, fetal bovine serum; IC₅₀, half-maximum inhibitory concentration values; PBS, phosphate buffered saline; PcAlCl, phthalocyanine aluminum chloride; PcAlS_{mix}, mixture of phthalocyanine compounds with different sulfonation degree, having formula PcAlOH(SO₃Na)_n with <n> ~ 3; PDT, photodynamic therapy; PI, propidium iodide; RM⁺, Rheinwalds's medium; RPMI, Roswell Park Memorial Institute; SDS, sodium dodecyl sulphate.

REFERENCES

- ¹(a) M. P. Donzello, D. Vittori, E. Viola, I. Manet, L. Mannina, L. Cellai, S. Monti, C. Ercolani, *Inorg. Chem.* 50 (2011) 7391-7402; (b) M. P. Donzello, E. Viola, C. Ercolani, Z. Fu, D. Futur, K. M. Kadish, *Inorg. Chem.* 51 (2012) 12548-12559.
- ²(a) P. Agostinis, K. Berg, K. A. Cengel, T. H. Foster, A.W. Girotti, S. O. Gollnick, S. M. Hahn, M. R. Hamblin, A. Juzeniene, D. Kessel, M. Korbelik, J. Moan, P. Mroz, D. Nowis, J. Piette, B. C. Wilson, J. Golab, *Ca-Cancer J. Clin.* 61 (2011) 250-281; (b) J. P. Celli, B. Q. Spring, I. Rizvi, C. L. Evans, K. S. Samkoe, S. Verma, B. W. Pogue, T. Hasan, *Chem. Rev.* 110 (2010) 2795-2838; (c) A. E. O'Connor, W. M. Gallagher, A. T. Byrne, *Photochem. Photobiol.*, 85 (2009) 1053-1074; (d) K. Szacilowski, W. Macyk, A. Drzewiecka-Matuszek, M. Brindell, G. Stochel, *Chem. Rev.* 105 (2005) 2647-2694.
- ³ (a) M. Machacek, A. Cidlina, V. Novakova, J. Svec, E. Rudolf, M. Miletin, R. Kučera, T. Simunek, P. Zimcik, *J. Med. Chem.* 58 (2015) 1736-1749; (b) S. Makhseed, M. Machacek, W. Alfady, A. Tuhl, M. Vinodh, T. Simunek, V. Novakova, P. Kubat, E. Rudolf, P. Zimcik, *Chem. Commun.* 49 (2013) 11149-11151; (c) T. Nyokong, *Coord. Chem. Rev.* 251 (2007) 1707-1722; (d) H. Shinohara, O. Tsaryova, G. Schnurpfeil, D. Wöhrle, *J. Photochem. Photobiol., A: Chemistry*, 184 (2006) 50-57; (e) R. W Redmond, J. N. Gamlin, *Photochem. Photobiol.*, 70 (1999) 391-475; (f) W. Spiller, H. Kliesch, D. Wöhrle., S. Hackbarth, B. Roder, G. Schnurpfeil, *J. Porphyrins Phthalocyanines*, 2 (1998) 145-158.
- ⁴ (a) Z. Musil, P. Zimcik, M. Miletin, K. Kopecky, P. Petrik, J. Lenco, *J. Photochem. Photobiol., A: Chemistry* 186 (2007) 316-322; (b) S. M. Baum, A. A. Trabanco, A. G. Montalban, A. S. Micallef, C. Zhong, H. G. Meunier, K. Suhling, D. Phillips, A. J. P. White, D. J. Williams, A. G. M. Barrett, B. M. Hoffman, *J. Org. Chem.* 68 (2003) 1665-1670; (c) E. G. Sakellariou, A. G. Montalban, H. Meunier, G. Rumbles, D. Philips, R. B. Ostier, K. Suhling, A. G. M. Barrett, B. M. Hoffman, *Inorg. Chem.* 41 (2002) 2182-2187; (d) U. Michelsen, H. Kliesch, G. Schnurpfeil, A. K. Sobbi, D. Wöhrle, *Photochem. Photobiol.* 64 (1996) 694-701.

-
- ⁵ (a) I. Manet, F. Manoli, M. P. Donzello, E. Viola, G. Andreano, A. Masi, L. Cellai, S. Monti, *Org. Biomol. Chem.* 9 (2011) 684-688; (b) I. Manet, F. Manoli, M. P. Donzello, C. Ercolani, D. Vittori, L. Cellai, A. Masi, S. Monti, *Inorg. Chem.* 50 (2011) 7403-7411.
- ⁶ I. Manet, F. Manoli, M. P. Donzello, E. Viola, A. Masi, G. Andreano, G. Ricciardi, A. Rosa, L. Cellai, C. Ercolani, S. Monti, *Inorg. Chem.* 52 (2013) 321-328.
- ⁷ N. A. Kuznetsova, N. S. Gretsova, V. M. Derkacheva, S. A. Mikhaleiko; L. I. Soloveva, O. A. Yuzhakova, O. L. Kaliya, E. A. Lukyanets, *Russ. J. Gen. Chem.* 72 (2002) 300-306.
- ⁸ E. A. Lukyanets, Organic Intermediates & Dyes Institute, Moscow 123995, Russia. E-mail: rmeluk@niopik.ru
- ⁹ C. Bergami, M. P. Donzello, F. Monacelli, C. Ercolani, K. M. Kadish, *Inorg. Chem.* 44 (2005) 9862-9873.
- ¹⁰ M. Ambroz, A. Beeby, S. MacRobert, M. S. C. Simpson, R. K. Svensen, D. Phillips, *J. Photochem. Photobiol. B: Biology* 9 (1991) 87-95.
- ¹¹ N. A. Kuznetsova, N. S. Gretsova, V. M. Derkacheva, O. L. Kaliya, E. A. Lukyanets, *J. Porphyrins Phthalocyanines* 7 (2003) 147-154.
- ¹² V. Nardello, D. Brault, P. Chavalle, J. M. Aubry, *J. Photochem. Photobiol. B: Biology* 29 (1997) 146-155.
- ¹³ N. A. Kuznetsova, N. S. Gretsova, O. A. Yuzhakova, V. M. Negrimovskii, O. L. Kaliya, E. A. Lukyanets, *Russ. J. Gen. Chem.* 71 (2001) 36-41.
- ¹⁴ M. P. Donzello, E. Viola, M. Giustini, C. Ercolani, F. Monacelli, *Dalton Trans.* 41 (2012) 6112-6121.
- ¹⁵ A. Chahti, M. Boukalouch, J. P. Dumas, A. El Kinani, *J. Disp. Sci. and Technology* 21 (2000) 525-535.
- ¹⁶ J. G. Rheinwald, *Methods for Clonal Growth and Serial Cultivation of Normal Human Epidermal Keratinocytes and Mesothelial Cells*, IRL Press, Oxford, 1989, pp. 81-94.
- ¹⁷ M. P. Donzello, D. Vittori, D. Futur, Z. Fu, C. Ercolani, K. M. Kadish, *J. Porphyrins Phthalocyanines* 17 (2014) 896-904.

-
- ¹⁸ T. Nyokong, E. Antunes, Photochemical and Photophysical Properties of Metallophthalocyanines in Handbook of Porphyrin Science 7 (2010) 247-357.
- ¹⁹ (a) J. M. Fernandez, M. D. Bilgin, L. I. Grossweiner, J. Photochem. Photobiol. B: Biol. 37 (1997) 131-140; (b) I. Rosenthal, C. Murali Krishna, P. Riesz, E. Ben-Hur, Rad. Research 107 (1986) 136-142; (c) J. Davila, A. Harriman, Photochem. Photobiol. 50 (1989) 29-35; (d) N. A. Kuznetsova, N. S. Gretsova, O. A. Yuzhakova, V. M. Negrimovskii, O. L. Kaliya, E. A. Lukyanets, Russ. J. Gen. Chem. 71 (2001) 36-41; (e) N. A. Kuznetsova, N. S. Gretsova, V. M. Derkacheva, S. A. Mikhalenko, L. I. Soloveva, O. A. Yuzhakova, O. L. Kaliya E. A. Lukyanets, Russ. J. Gen. Chem. 72 (2002) 300-306; (f) A. Ogunsipe, T. Nyokong, J. Porphyrins Phthalocyanines 9 (2005) 121-129.
- ²⁰ C. Marti, S. Nonell, M. Nicolau, T. Torres, Photochem. Photobiol. 7 (2000) 53-59.
- ²¹ H. Abramczyk, B. Brozek-Pluska, M. Tondusson, E. Freysz, J. Phys. Chem. C 117 (2013) 4999-5013.
- ²² R. M. Amin, C. Hauser, I. Kinzler, A. Rueck, C. Scalfi-Happ, Photochem. Photobiol. Sci. 11 (2012) 1156-1163.
- ²³ C. M. Lerche, S. Fabricius, P.A. Philipsen, H. C. Wulf, Photochem. Photobiol. Sci. 14 (2015) 875-882.